ISSN 1392 - 1207. MECHANIKA. 2010. Nr.5(85)

Investigation of resistance of nuclear fuel cladding to hydride cracking

V. Makarevičius*, A. Grybėnas, R. Kriūkienė*****
**Lithuanian Energy Institute, Breslaujos 3, 44403 Kaunas, Lithuania, E-mail: makarev@mail.lei.lt*
***Lithuanian Energy Institute, Breslaujos 3, 44403 Kaunas, Lithuania, E-mail: grybenas@mail.lei.lt*
****Lithuanian Energy Institute, Breslaujos 3, 44403 Kaunas, Lithuania, E-mail: rita@mail.lei.lt*

1. Introduction

Zirconium alloys are used as structural materials for nuclear reactors. This is due to a combination of the properties such as strength and ductility at reactor-operating temperatures, good corrosion resistance at high temperatures and compatibility with fuel materials. Zirconium alloys are widely used for manufacturing of fuel claddings, fuel spacer grids, pressure tubes and control rods. However, zirconium, similar like titanium alloys are susceptible to hydrogen [1, 2]. Zirconium phase has a very low solubility of hydrogen, resulting in any excess hydrogen getting precipitated as zirconium hydride. This leads to embrittlement [3], delayed hydride cracking (DHC) and hydride blistering, all of which limit the lifetime of reactors and cause serious safety and environmental concerns.

DHC is a phenomenon where a crack can propagate in stepwise fashion as a result of hydrogen redistribution ahead of the crack tip under a stress level below the yield stress. The high mobility of hydrogen enables hydride to redistribute. If stress levels are sufficiently high and local hydrogen concentration exceeds the terminal solid solubility, hydride platelets precipitate in the primary cracking direction. When a platelet reaches a critical length, it cannot support the local stress and it ruptures. The crack advances this distance and it arrests in the fracture resistant zirconium matrix. Repetition of this process causes continued cracking [1].

The necessary conditions for DHC are the presence of a crack, a sufficiently high hydrogen concentration, tensile stresses and a stress intensity factor (K_I) larger than the threshold value at the crack tip. The latter condition is called K_{IH}, - the critical stress intensity factor in the presence of hydride, below which no crack growth occurs. At K_I values above K_{IH} the rate of cracking, V, is essentially independent of K_I.

DHC has been identified as the cause of failure of pressure tubes in both CANDU and RBMK reactors [4, 5]. Although the failures of the pressure tubes have had the highest technological significance, DHC can be responsible for failures in other components, as guide tubes for control rods and fuel claddings. Conditions for DHC can appear in fuel claddings during reactor operation and storage of spent nuclear fuel [6]. Residual tensile stresses at welds can provide the driving force for growth of the hydrides. It was reported [7] failure of unirradiated Zr-2.5Nb fuel rods after long-term storage at room temperature.

In some zircaloy nuclear fuel cladding used in boiling-water reactors (BWR), hydride cracking was found in the form of long splits that allowed substantial leakage of fission products [8]. Cladding in BWR's is usually a tube with the diameter of about 10 mm, wall thickness of about 0.6 mm and length of about 4 m. If the cladding wall is penetrated during operation, for example by fretting, water from the heat-transport system can enter into the fuel rod gap where steam is produced. Much hydrogen is generated because the steam oxidizes the fuel and the inside surface of the cladding, reducing the partial pressure of oxygen and leaving a gas rich in hydrogen. At some distance from the primary defect the gas becomes almost pure hydrogen, and with breakdown of the protective oxide layer, copious quantities of hydrogen may be absorbed by the cladding. With fuel expansion during power ramping, the hydrided cladding is stressed, which leads to crack initiation. The cracks grow through-wall and may be over 1 m long. The fractures are characterized by brittle regions in "striations" or "chevrons", with the crack front often leading towards the outside surface of the cladding. The mechanism of cracking appears to be a form of DHC perhaps exacerbated by a continuous additional supply of hydrogen from the steam inside the fuel element [9]. The design of the RBMK reactor fuel differs little from fuel elements manufactured for standard BWR-type reactors [10]. Fuel assembly of RBMK-1500 used in Ignalina NPP contains 18 fuel elements arranged within two concentric rings in a central carrier rod. RBMK-1500 core contains 1661 fuelled channels.

While the main reported problems for RBMK-1500 fuel assemblies was corrosion of the fuel channels and assemblies, corrosion sludge can cause circulation problems and as a consequence local overheating and depressurization of fuel assemblies.

The aim of this work was investigate resistance to hydrogen induced cracking of zirconium fuel cladding materials prepared at different thermal treatment conditions.

2. Experimental program

Zircaloy-4 cladding tubes from two different batches manufactured by Sandvik Steel AB were used for testing. The properties of SANDVIK Zr-4 lot 86080 and 83786 cladding tubes are shown in Table 1.

Table 1

Properties of SANDVIK Zr-4 cladding tube

	Lot 86080	Lot 83786
Outer diameter, mm	9.50	9.52
Wall thickness, mm	0.57	0.595
Yield Strength (RT), MPa	548 - 558	586-592
Tensile Strength (RT), MPa	757 - 759	755-782
Elongation (RT),%	18 - 20	16
Yield Strength (385°C), MPa	356 - 355	365-375
Tensile Strength (385°C), MPa	439 - 458	466
Elongation (385°C), %	21 - 19	16-18

Initial cold-worked (CW) tube samples were heat treated in Studsvik [11] at the temperature/time parameters typical for PWR and BWR cladding to produce materials in cold-worked stress-relieved (CWSR) and recrystallized (RXA) condition. Sample numbering of different cladding tubes is in Table 2.

Table 2

Samples of cladding tubing

Lot No	86080	83786		
Sample No	LT_S7	51	52	53
Thermal treatment	480°C / 3.5h	-	480°C / 3.5h	565°C / 1.5h
Condition	CWSR	CW	CWSR	RXA
Outer diameter (mm)	9.50	9.52		
Wall thickness (mm)	0.57	0.595		

Cladding pieces with a length of 220 mm in length were electrolytically hydrided at current density 1.5 kA/m^2 for 12 h at 70°C to produce a hydride layer of about 10-12 μm at the outer surface of the tube. Hydrided pieces were then heat treated at 410°C during 24 hours to obtain about 200 wt-ppm average hydrogen concentration in the bulk of material. Calculation of hydride layer thickness, necessary homogenization time and temperature to produce specimens with required hydrogen concentration is described in [12, 13].

From the hydrided cladding tube sections sharply notched test specimens were manufactured. The specimens have a length of 13 mm and are axially notched at both edges. The notch width at the front edge of the specimen is 0.2 mm and the notch width of 0.5 mm is used for the back edge. The axial notches at the front were extended by fatigue precracking at room temperature up to 1.5- 1.6 mm in length. Fatigue precracking was performed on a Model 2055P-05 modified testing machine with a frequency of loading 1.6 Hz. Crack increase was monitored by direct observation according to reference lines drawn on both sides of the specimen, using microscope with magnification 10X. The specimens have been fatigue precracked starting at maximum loads of 200 N, gradually decreasing maximum load to 100 N. After precracking, the total length, a^* (Fig. 1), including the machined notch, was about 2.5-3 mm.

Delayed hydride cracking velocity in cladding specimens was determined using pin loading tension (PLT) technique. The PLT test was developed for evaluation of the fracture toughness of thin-walled tubing [11, 14, 15]. The PLT-fixture consists of two halves, which together form the cylindrical holder (Fig. 2). This cylindrical holder has a diameter, which allows it to be inserted into the tubular PLT-specimen, while maintaining a minimal interfacial gap. The fixtures are manufactured from heat resistant alloy.

The specimen and fixture have closely interrelated configurations and when combined, create an assembly (Fig. 2) characterised by the ratio W/a, where W is the distance between the load-line and the rotation axis of the fixture halves, and a is the distance between the load-line and the notch tip in the specimen. The fixture used for testing have the parameters S = 8 mm and W = 19 mm.

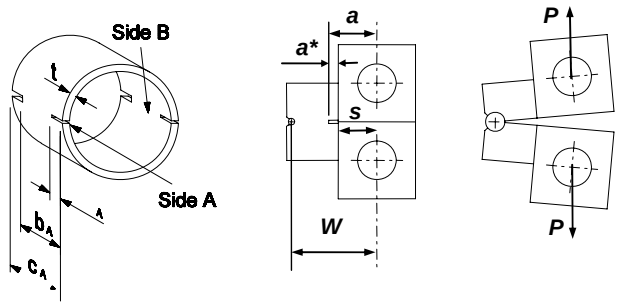

Fig. 1 Specimen and specimen-fixture geometry for PLT testing: a^* = front notch (crack) in the specimen; S = dimensional parameter of the fixture; W = distance between the loading line and the rotation axis; $a = a^* + S$ = crack length for specimen-fixture assembly

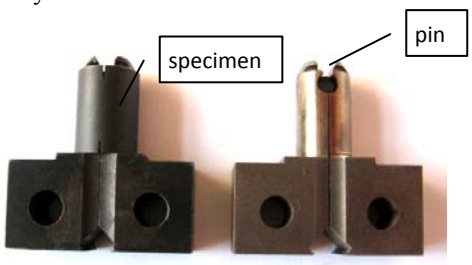

Fig 2 PLT-fixtures and a 13 mm specimen

DHC testing was performed on machine IMAS-20, modified with suitable pull rods and adapters. The machine is equipped with an electric furnace suitable for long - time heating of small specimens up to about 400 °C. Programmable temperature controller allows to maintain heating and cooling of the test specimen at a given rates. During DHC testing actual test temperature and pre-set temperature (temperature programme) readings are recorded to computer data file (logging period 1 sec.). Temperature measurements were performed using K-type thermocouple mounted on the PLT specimen.

Crack propagation during DHC test was monitored by the evaluation of specimen opening because there is a correlation of displacement increase during DHC with the final crack length (Fig. 3). Load-line displacement measurements were carried out using Mitutoyo Digimatic indicator 543-690B connected to a PC using interface DMX-1. Displacement readings were registered every 12 s. To increase sensitivity, the indicator was mounted using mechanical lever with arm moving ratio 1:4.5.

DHC testing is sensitive to the temperature history, the maximum value is attained by cooling from a temperature higher than the solvus temperature of hydrogen in the specimen, and therefore a temperature cycle was applied to all specimens before testing. The specimens were heated at 5°C per min to a peak temperature, soaked for 1h and cooled down at 1.5°C per min to the test temperature and soaked for about 50 min before loading. Peak temperature was selected at least 50°C above the test temperature.

A temperature-time schedule is illustrated in Fig. 4 and peak and test temperatures are shown in Table 3.

To define the difference between the temperatures inside the furnace, temperatures were measured at the adapter and at the specimen using additional thermocouple.

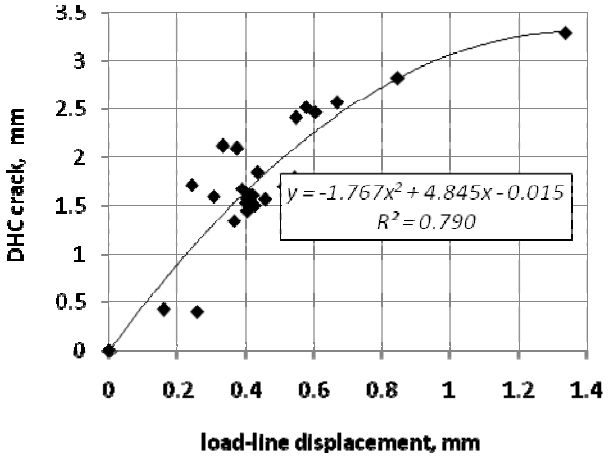

Fig. 3 DHC crack length plotted versus corresponding load line displacement values

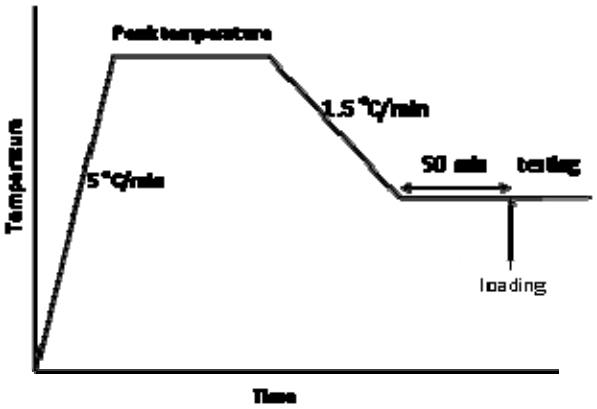

Fig. 4 Temperature-time schedule for the DHC testing

Table 3

Peak and test temperatures for DHC testing

Peak temperature, °C	Test temperature, °C
333	283
333	279
333	275
315	250
285	200
275	144

Temperature variations were within 1°C at the test temperature 250°C.

The precracked specimen is heated and after the specified thermal cycle it is loaded to apply an initial K_I of about 15 MPa·m^{½}. The load of 150 N is applied when the temperature is stabilized after the heating-cooling steps. The exact initial and final K_I values are calculated after the DHC test when the crack lengths are measured on the fracture surfaces. Necessary loading force to the specimen is applied with the set of calibrated weights.

The moment of crack initiation, t_0, was detected by increase in specimen opening. Cracking is allowed to continue until the crack has grown about 1.5-2.5 mm. The load is then removed or decreased to 30 N, the furnace is switched off and the specimen is cooled down to the room temperature while it remains in the furnace.

After the DHC-test is completed and the specimen is cooled to room temperature, fatigue precracking is performed at room temperature before opening the specimen to mark the end of the DHC-crack and the two halves of the cracked specimen are pulled apart.

Fractured specimen has been photographed using computerised image analysis system.

Two fracture surfaces are observed at each half of the PLT-specimen after opening: Side A and Side B (Fig. 5). The length of the DHC crack is calculated for each side of the specimen as the difference between the average final crack length, a_F, after DHC test, and the average crack length after fatigue precracking, a_0. The average values for each specimen side are obtained by means of a 9-point averaging method.

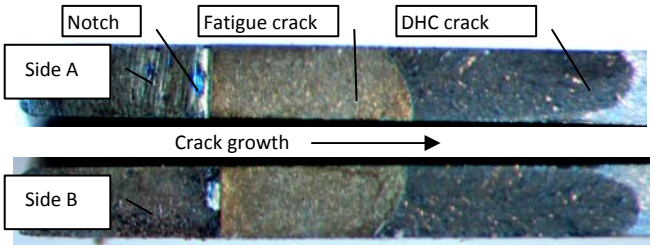

Fig. 5 Area method for average DHC length measurement from fractured surface of CCT specimen

An effective crack length, a, in the PLT-specimen is characterised as an average of the corresponding values measured at the two fracture surfaces. Thus, the DHC crack extension, a_{DHC}, in the PLT specimen is characterised as

$$a_{DHC} = a_F - a_0 \quad (1)$$

where an effective crack length after fatigue precracking or initial crack, a_0, and an effective crack after DHC test or final crack, a_F, are calculated for each specimen as $0.5(a_A + a_B)$.

The K_I -values are calculated using the following equation:

$$K_I = [P / (2t\sqrt{W})]f(a/W) \quad (2)$$

where P is the load applied to specimen, N; t is wall thickness of the cladding, m, W is width of the specimen-fixture assembly, m; a = effective crack length, m. The specimen geometry factor $f(a/W)$ is determined experimentally from compliance measurements [11]

$$f(a/W) = -360.99(a/W)^3 + 787.15(a/W)^2 -$$

$$- 468.73(a/W) + 92.203 \quad (3)$$

$$a \text{ (mm)} = a^* + 8\cdot10^{-3} \text{ (see Fig. 1)} \quad (4)$$

An average DHC crack velocity, V_{DHC}, is calculated from the DHC crack length, a_{DHC}, measured on the specimen fracture surfaces and the time, t_{DHC}, needed for crack growth

$$V_{DHC} \text{ (m/s)} = a_{DHC}10^{-3}/(60\cdot t_{DHC}) \quad (5)$$

where t_{DHC} (min) = $t_F - t_0 - t_{INC}$ is calculated as difference $t_L - t_{INC}$, between time on load, t_L,= $t_F - t_0$, and incubation time, t_{INC} , where the incubation time is the time on load before crack growth initiation.

3. Results and discussion

Microstructure of the tested material was revealed by etching in composition of H_2SO_4: HNO_3: HF: H_2O (3: 3: 1: 3). Metallography of hydride structure on radial-axial and radial-transverse sections shows a uniform hydride distribution with hydrides elongated in the longitudinal direction (Fig. 6). The length of the hydrides is generally less than 200 μm, thickness is about 3 μm. CW and CWSR material microstructure is similar. Hydrides in the RXA material are arranged more chaotically (Fig. 7).

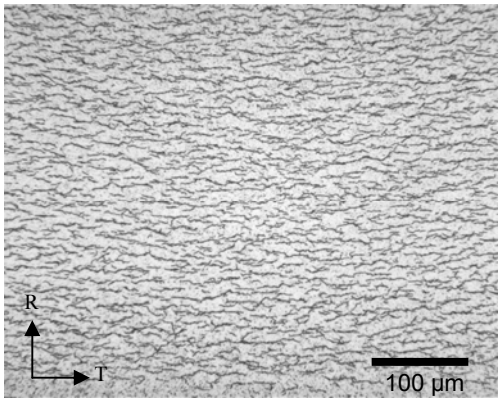

Fig. 6 Hydride microstructure of the radial-transverse section of cold-worked Zircaloy-4 cladding tube material

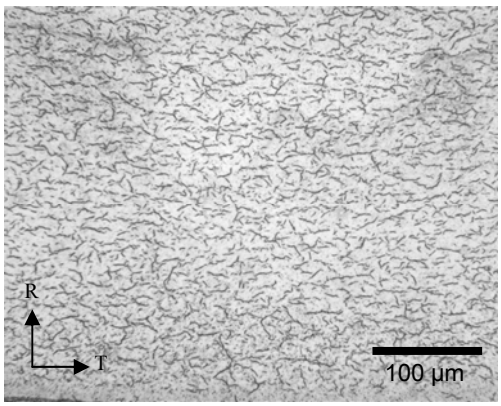

Fig. 7 Hydride microstructure of radial-transverse section of the recrystallized Zircaloy-4 cladding tube material

Cladding specimens show different DHC behavior depending on material heat treatment condition. The DHC velocity values at 250°C for eight tested specimens of CWSR material are within interval from 3.28×10^{-8} m/s to 4.15×10^{-8} m/s with an average value 3.67×10^{-8} m/s. Confidence interval (95.0%) for mean is 2.65×10^{-9} m/s. Crack growth velocity of CW material differs from 5.72×10^{-8} m/s to 6.26×10^{-8} m/s with an average value 6.02×10^{-8} m/s. Fig. 8 shows DHC axial velocity data at 250°C for the CWSR cladding specimens compared to CW material.

Lot 8378 CWSR specimens were also tested at 144, 200, 275, 279 and 283°C. Maximum DHC rate values were found at 275°C, but DHC velocity sharply decreases at temperatures above 275°C. Limited or no cracking is observed at 283°C and above. Temperature dependence of DHC axial velocity of CWSR cladding is shown in Fig. 9. DHC velocity of CWSR cladding in a temperature range 144 - 275°C follows Arrhenius relationship

$$V_{DHC} = 0.0211 exp(-6.943(1000/T)) \quad (7)$$

RXA material shows no cracking at 250°C and low DHC velocity at 200°C. After 41 days of test at 200°C, calculated DHC velocity was $7.89\cdot10^{-11}$ m/s.

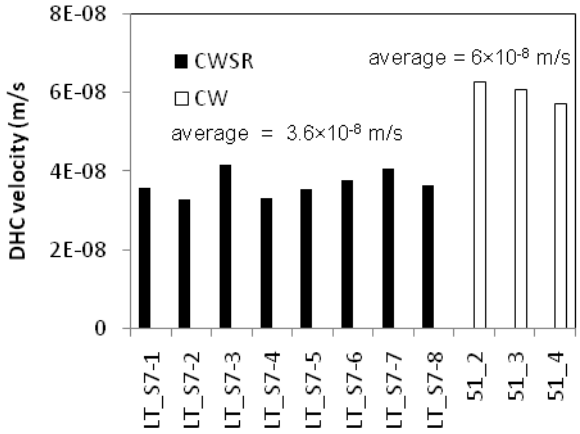

Fig. 8 DHC axial velocity at 250 °C for the cladding with CW and CWSR thermal treatment

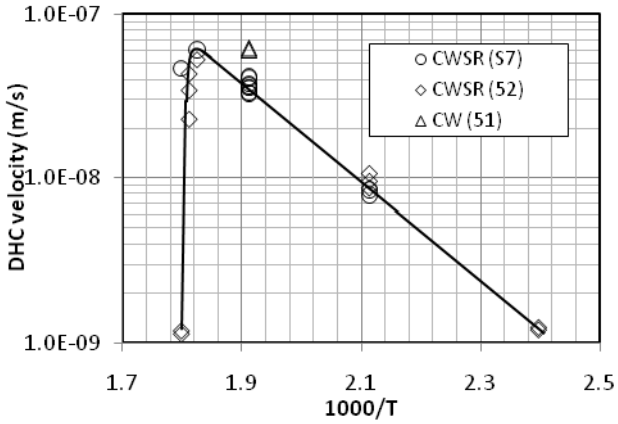

Fig. 9 Temperature dependence of DHC axial velocity of CWSR cladding Lot 8378

The DHC velocity values at 250°C for eight tested cladding tube specimens are within interval from $3.28\cdot10^{-8}$ to $4.15\cdot10^{-8}$ m/s are shown in Table 4. These values are similar to the crack velocities obtained earlier for RBMK TMT-1 material and are about 2.5 times lower than the values for CANDU pressure tube [16].

Incubation times are quite variable, ranging from 42 to 170 min. As fatigue precracking and DHC testing was performed on different testing machines, a possible explanation for the large incubation times could be specimen relocation on the fixture when the specimen is replaced from precracking machine to DHC testing machine. Relocation of the specimen on fixture can affect the stress state at the crack tip. Load-line displacement measurement allows the determination of incubation time with high accuracy; therefore it cannot contribute a significant error to DHC measurement. There is a correlation with the final crack length (Fig. 3) and therefore prediction of the crack length is possible. However, it is difficult to estimate crack growth in RXA cladding due to large crack opening because of plastic deformation.

DHC velocity of CWSR cladding follows Arrhenius relationship up to 275°C, but at higher temperatures sharply decreases. This temperature limit for CWSR zircaloy cladding is much lower than in case of Zr-2.5Nb pressure tube materials. It is known [16] that temperature limit for delayed hydride cracking in Zr-2.5Nb alloys is from 300 to 310°C.

Table 4
Statistical parameters of DHC velocity test results at 250°C

Number of specimens	8
Minimum	3.28E-08 m/s
Maximum	4.15E-08
Mean	3.67E-08
Median	3.61E-08
Standard Error	1.12E-09
Standard Deviation	3.17E-09
Range	8.64E-09
Confidence interval for mean (95.0%)	2.65E-09

DHC velocity in CW material shows good coincidence of results. DHC rate is about 1.6 times higher than in stress relieved material.

BWR (RXA) material at 250°C shows no obvious cracking. Load line – displacement curve shows unusual crack opening during the initial phase of testing, but no observable crack was found on the fracture surface. Testing at 200°C revealed that after 41 days on load, measured DHC crack length on the fracture surface was only 0.28 mm. Calculated DHC velocity was $7.89 \cdot 10^{-11}$ m/s, that is more than one hundred times slower, than DHC velocity in CWSR cladding at 200°C.

CWSR materials from different lots show similar DHC values (Fig. 9).

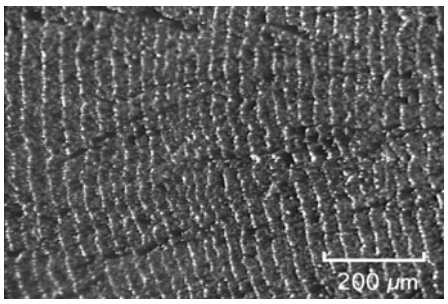

Fig. 10 Striations on the DHC fracture surface of Zr-2.5Nb [16]

Fracture surface of the cladding material is different from Zr-2.5Nb pressure tube material; the fractographic features called striations were absent. The propagation of a crack in Zr-2.5Nb creates lines on the fracture surface, which lie parallel to the crack front, perpendicular to the direction of crack growth. Each incremental advance of the crack front results in the formation of a striation on the fracture surface (Fig. 10). Probable reason for the absence of striations in zircaloy is smaller steps in DHC crack front propagation due to different microstructure.

Despite fractographic differences DHC velocity values in CWSR cladding material are comparable to the crack velocities for Zr-2.5Nb alloys [16, 17]. DHC velocity depends mainly on texture, microstructure and yield stress [18]. Variation of these parameters can explain DHC behaviour in cladding materials with different heat treatment condition.

4. Conclusions

1. Samples of unirradiated cladding tubing in different heat treatment conditions (CW, CWSR, RXA) containing about 200 ppm of hydrogen were tested for delayed hydride cracking velocity in a temperature range 144-283°C.
2. It was found, that up to 275°C DHC velocity follows Arrhenius relationship, at higher temperatures DHC velocity sharply decreases.
3. DHC velocity differs depending on the material heat treatment conditions. At 250°C cracking velocity in CW material was found about 1.6 times higher than in CWSR cladding and no cracking was observed in RXA material.
4. Although DHC velocity values in fuel claddings are comparable to those in Zr-2.5Nb pressure tube materials, fractographic features called striations were absent in all tested cladding materials.

Acknowledgements

The authors acknowledge Lithuanian Science and Study Foundation for providing support.

References

1. **Amouzuovi, K.F., Clegg, L.J.** Effect of heat treatment on delayed hydride cracking in Zr-2.5Nb wt pct Nb. -Metallurgical Transactions, v.18A, 1987, p.1687-1694.
2. **Medekshas, H.** Effect of elevated temperature and welding on low cycle fatigue strength of titanium alloys. -Mechanika. -Kaunas: Technologija, 2008, Nr.2(70), p.5-10.
3. **Janulionis, R. Daunys, M. Dundulis, G. Grybėnas, A. Karalevičius, R.** Numerical and experimental research of the influence of hydrogen on the fracture toughness of zirconium – 2.5% niobium alloy. -Mechanika. -Kaunas: Technologija, 2008. Nr.6(74), p.5-10.
4. **Cheadle, B.A., Coleman, C.E., Rodgers, D.K., Davies, P.H., Chow, C.K. and Griffits, M.** Examination of core components removed from CANDU reactors international. -Conference on CANDU Maintenance, Canadian Nuclear Society November 1998, 13p.
5. Safety Assessment of Proposed Modifications for Ignalina Nuclear Power Plant IAEA-EBP-RBMK-03. IAEA, Vienna, 1995.
6. **Kim Y.S.** Delayed hydride cracking of spent fuel rods in dry storage. -Journal of Nuclear Materials, 2008, v.378, p.30-34.
7. **Simpson, C.J., Ells, C.E.** Delayed hydrogen embrittlement in Zr-2.5 wt % Nb. -Journal of Nuclear Materials, 1974, v.52, p.289-295.
8. **Grigoriev, V., Jakobsson, R.** Delayed hydrogen cracking velocity and J-integral measurements on irradiated BWR cladding. -Journal of ASTM International, 2005, v.2, Iss.8, 16 p.
9. **Edsinger, K., Davies, J.H., Adamson, R.B.** Degraded fuel cladding fractography and fracture behavior, -Zirconium in the Nuclear Industry. 12th International

Symposium, ASTM STP 1354, eds. G.P. Sabol and G.D. Moan, ASTM,West Conshohocken, PA., 2000: p.316-339.
10. **Almenas, K., Kaliatka, A., Uspuras, E**. Ignalina RBMK-1500. A Source Book: extended and updated version. -Kaunas, 1998.-198 p.
11. **Grigoriev, V., Jakobsson, R.** DHC Axial Crack Velocity Measurements in Zirconium Alloy Fuel Cladding. -Pin-Loading Tension (PLT) *Test* Procedure for IAEA Round Robin Test Program. STUDSVIK/N-05/281. Studsvik Nuclear AB, Nyköping, Sweden, 2005.-24 p.
12. **Lepage, A.D., Ferris, W.A. and Ledoux, G.A.** Procedure for Adding Hydrogen to Small Sections of Zirconium Alloys. AECL Report No. FC-IAEA-03, T1.20.13-CAN-27363-03, 1998 November.
13. **Makarevičius, V., Grybėnas, A., Levinskas, R.** Controlled hydriding of Zr-2,5%Nb alloy by thermal diffusion. -Materials Science (Medžiagotyra), 2001, v.7(4), p.249-251.
14. **Grigoriev, V., Josefsson, B., Lind, A., Rosborg, B.** A Pin-loading tension test for evaluation of thin-walled tubular materials. -Scripta Metallurgica et Materialia, 1995, v.33, p. 109-114.
15. **Grigoriev, V., Josefsson, B., Rosborg, B., Baj, J.,** A novel fracture toughness testing method for irradiated tubing. Experimental results and 3D numerical modelling. -Transactions of the 14th International Conference on Structural Mechanics in Reactor Technology (SMiRT-14), 1997, Vol. 2. p.57-64.
16. **Grybenas, A., Makarevicius, V., Dundulis, G**. Effect of test temperature and load ratio on hydride cracking rate of Zr-2.5Nb alloy. -Mechanika. -Kaunas: Technologija, 2007, Nr.1(63), p.21-26.
17. Delayed hydride cracking in zirconium alloys in pressure tube nuclear reactors. -Final report of coordinated research project. 1996-2002. IAEA-TECDOC-1410, October 2004, Vienna.
18. **Oh, J.Y., Kim, I.S., Kim, Y.S.** A normalization method for relationship between yield stress and delayed hydride cracking velocity in Zr-2.5Nb alloys. -Journal of Nuclear Science and Technology, 2000, v.37, No7, p.595-600.

V. Makarevičius, A. Grybėnas, R. Kriūkienė

BRANDUOLINIO KURO APVALKALO ATSPARUMO HIDRIDINIAM PLEIŠĖJIMUI TYRIMAS

R e z i u m ė

Darbe tiriama vandenilio įtaka plyšių susidarymui šiluminių elementų lydinio „Zircaloy-4“ apvalkaluose. Nustatyta temperatūros ir terminio apdirbimo įtaka lėto hidridinio plyšimo (LHP) greičiui. Įhidrinus apvalkalo medžiagą iki 200 ppm vandenilio koncentracijos, specialios konstrukcijos bandiniuose suformavus nuovargio plyšį, buvo nustatomas LHP greitis 144 – 283°C temperatūrų intervale, esant įtempių koncentracijos koeficientui K_I apie 15 MPa√m. Kylant temperatūrai iki 275°C, LHP greitis didėja pagal Arenijaus priklausomybę, aukštesnėje temperatūroje LHP greitis staigiai mažėja. LHP greitis priklauso nuo kuro apvalkalo medžiagos terminio apdirbimo režimo. LHP greitis šaltai apdirbtoje medžiagoje yra apie 1,6 karto didesnis nei termiškai atleistame lydinyje; rekristalizuotame lydinyje LHP nevyksta.

V. Makarevičius, A. Grybėnas, R. Kriūkienė

INVESTIGATION OF RESISTANCE OF NUCLEAR FUEL CLADDING TO HYDRIDE CRACKING

S u m m a r y

In this study hydride induced cracking was investigated using specimens prepared from Zircaloy-4 fuel cladding materials. Temperature dependence of the delayed hydride cracking (DHC) rate and the influence of heat treatment on hydride cracking was evaluated. After adding about 200 wt-ppm of hydrogen to the samples DHC velocity was determined on fatigue precracked specimens using pin-loading tension technique. Tests were done under constant loading and initial K_I value of about 15 MPa√m. Crack growth velocity was determined at temperature range 144- 283°C. It was found that cracking velocity has Arrhenius type temperature dependence and increases up to 275 °C, at higher temperatures cracking rate sharply decreases. Delayed hydride cracking velocity depends on thermal treatment conditions of the cladding material, DHC rate is about 1.6 times higher in cold-worked than in stress-relieved material and no cracking was observed in recrystallized material.

В. Макарявичюс, А. Грибенас, Р. Крюкиене

ИССЛЕДОВАНИЕ ОБОЛОЧКИ ЯДЕРНОГО ТОПЛИВА НА ГИДРИДНОЕ РАСТРЕСКИВАНИЕ

Р е з ю м е

В работе исследуется влияние водорода на образование трещин в оболочке тепловыделяющих элементов сплава Zircaloy-4. Установлено влияние температуры и термической обработки на скорость замедленного гидридного растрескивания (ЗГР). После ввода в сплав 200 ppm водорода, были изготовлены образцы специальной конструкции, в которых сформирована усталостная трещина. Скорость ЗГР установлена при коэффициенте концентрации напряжений K_I = 15 MPa√m. Скорость замедленного гидридного растрескивания установлена в температурном интервале 144 - 283°C. С увеличением температуры до 275°C скорость ЗГР увеличивается по зависимости Аррениуса, при более высокой температуре скорость ЗГР быстро снижается. Скорость ЗГР зависит от термической обработки материала оболочки тепловыделяющих элементов. В материале с холодной обработкой скорость ЗГР в 1.6 раза превышает ЗГР в термически отпущенном сплаве, в рекристаллизованном сплаве ЗГР не происходит.

Received May 28, 2010
Accepted September 27, 2010